

Apelin/APJ alleviates diabetic nephropathy by improving glomerular endothelial cells dysfunction via SIRT3-KLF15

MINGCONG HUANG¹, JING CHANG², YU LIU¹, JIMING YIN³ and XIANGJUN ZENG¹

¹Department of Physiology and Pathophysiology, Capital Medical University, Beijing 100069, P.R. China;

²Department of Physiology, Beijing You An Hospital, Capital Medical University, Beijing 100069, P.R. China;

³Beijing Institute of Hepatology, Beijing You An Hospital, Capital Medical University, Beijing 100069, P.R. China

Received October 17, 2024; Accepted January 7, 2025

DOI: 10.3892/mmr.2025.13487

Abstract. Glomerular basement membrane (GBM) thickening, the earliest morphological change of diabetic nephropathy (DN), is related to glomerular endothelial cells (GECs) dysfunction which increase extracellular matrix (ECM) synthesizing. Apelin, the endogenous ligand for apelin/apelin receptor (APJ), is reported to alleviate endothelial cell dysfunction in DN. Therefore, it was hypothesized that apelin/APJ reduced GBM thickening by decreasing the synthesis of ECM in GECs. The results showed that apelin reduced glomerular fibrosis and GBM thickening by decreasing the expression of laminin and collagen IV in diabetic mice, which were cancelled following APJ knockout in GECs. Furthermore, apelin/APJ inhibited the synthesis of laminin and collagen IV in GECs by increasing the expression and activity of SIRT3, which promoted KLF15 deacetylation and translocation into nucleus. In conclusion, apelin/APJ reduced GBM thickening in diabetes mellitus by preventing laminin and collagen IV synthesizing via SIRT3-KLF15 pathway in GECs.

Introduction

Diabetic nephropathy (DN), as one of the most common and serious complications during diabetes mellitus (DM), is a major contributor to the diabetes-associated medical burden (1,2). During the development of DN, glomerular basement membrane (GBM) thickening is the earliest morphological change (2), which is associated with imbalanced

synthesis and degradation of extracellular matrix (ECM) (3-5) in glomerular endothelial cells (GECs) (6-8) and leads to renal dysfunction (3,9,10). Elucidating the mechanisms of GECs dysfunction will therefore aid in the understanding of GBM thickening in DN.

It has been reported that GECs-synthesized laminin and collagen IV are the main components which cause GBM thickening as a result of hyperglycemia and insulin resistance (3,11). However, hyperglycemia and insulin resistance cannot explain all GECs dysfunction during DM, because the strict control of these conditions does not necessarily prevent or slow down the disease progression (12). Increased adipokines as a result of DM-associated obesity have therefore attracted attention because they may directly affect endothelial cell function during DM (13,14). Apelin, an adipokine, is reported to improve endothelial cell dysfunction during DM (15,16), however whether it reduces GBM thickening remains unknown. It may be possible that apelin decreases ECM synthesis by alleviating GECs dysfunction during DM.

Synthesis and degradation of ECM in GECs both contributed to GBM thickening, however the synthesis controlled by transcription and translation plays a more critical role in the process of diabetic GBM thickening compared to the degradation (4,17). Therefore, it was hypothesized that apelin might decrease ECM synthesis in GECs during DM. What might be the intracellular mechanisms?

When tracing the intracellular signaling pathways for apelin, sirtuin-3 (SIRT3), downstream of apelin/apelin receptor (APJ) (18,19), was found to deacetylate Krüppel-like factor 15 (KLF15, an antifibrotic transcription factor), in a NAD⁺ dependent manner in MPC-5 cells (20). Moreover, KLF15 has been reported to inhibit type IV collagen and fibronectin expression in both podocytes and mesangial cells (21,22). However, whether SIRT3 regulates KLF15 in diabetes nephropathy and whether KLF15 controls laminin and type IV collagen transcription of in GECs, has not yet been reported. Therefore, it was hypothesized that apelin might prevent laminin and type IV collagen synthesis in GECs via SIRT3-induced KLF15 deacetylation and translocation into nucleus, thus reducing GBM thickening in the early phase of DN. Endothelial-specific APJ knockout mice were bred using Cre-loxP system to confirm whether apelin improved GBM thickening by directly binding to endothelial APJ.

Correspondence to: Professor Xiangjun Zeng, Department of Physiology and Pathophysiology, Capital Medical University, 10 You An men Wai Xi Tou Tiao, Beijing 100069, P.R. China
E-mail: megan_zeng@163.com

Dr Jiming Yin, Beijing Institute of Hepatology, Beijing You An Hospital, Capital Medical University, 8 You An men Wai Xi Tou Tiao, Beijing 100069, P.R. China
E-mail: yinjm7411@163.com

Key words: diabetic nephropathy, glomerular basement membrane, endothelial cells, extracellular matrix, apelin

Materials and methods

Animal models. All animal experiments were approved by the Ethics Committee of Capital Medical University and followed the guidelines established by the National Institutes of Health. APJ^{fl/fl} C57BL/6 mice (acquired from Knockout Mouse Project; The Jackson Laboratory) and TEK-CRE C57BL/6 mice (Cyagen Biosciences Inc.) aged 6-8 weeks were used. Endothelial-specific APJ knockout (APJ^{AEC}) mice were bred by crossing APJ^{fl/fl} mice and TEK-CRE mice in the Laboratory of Animal Experiments, Capital Medical University (Beijing, China). All animals were housed in specific pathogen-free animal quarters with 12 h light/dark cycle at a temperature of 21°C and 60% relative humidity. All the animal experiments were approved by the Ethics Committee for Animal Experiments of Capital Medical University (approval no. AEEI-2020-045) and according to the Guide for the Care and Use of Laboratory Animals (National Institutes of Health, <https://olaw.nih.gov/policies-laws/guide-care-use-lab-animals>).

A total of 24 male APJ^{fl/fl} mice and 24 APJ^{AEC} male mice (body weight: 23.57±0.19 g) were both randomly divided into sham group which were injected intraperitoneally with saline for 5 consecutive days (n=6); apelin treatment group which were injected intraperitoneally with saline for 5 consecutive days followed by intraperitoneally infusing (using micro-osmotic pump formalzet; Model 1004; DURECT Corporation) apelin-13 (30 µg/kg/day) for 4 weeks (n=6); streptozotocin (STZ) treatment group which were injected intraperitoneally with STZ (40 mg/kg/day) for 5 consecutive days (n=6); STZ + apelin treatment group which were injected intraperitoneally with STZ (40 mg/kg/day) for 5 consecutive days followed intraperitoneally infusing apelin-13 (30 µg/kg/day) for 4 weeks (n=6).

Animal health and behavior were monitored daily. Random blood glucose was measured every 5 days. Successful DM was confirmed if the random blood glucose increased to >16.0 mmol/l. During the experiment, no animals reached the humane endpoint of weight loss ≥15% within 5 weeks. After ~5 weeks treatment, a total of 48 mice were sacrificed via CO₂ inhalation for tissue collection and animal death was verified by observing indicators such as breath, heartbeat and nerve reflexes.

Immunohistochemistry (IHC) staining. Following sacrifice, kidneys of mice were harvested for histology. Kidney tissues were fixed with 10% formalin at room temperature for 24 h and embedded in paraffin after alcohol-xylene processed, then sectioned at the coronal plane. Tissue sections of 4 µm were treated with 3% H₂O₂ at room temperature for 15 min after antigen retrieval, then incubated with the primary antibody (4°C overnight) and HRP-conjugated secondary antibodies (room temperature for 1 h), followed by colorimetric detection using a DAB kit [cat. no. GK600705; GeneTech (Shanghai) Co., Ltd.] at room temperature for 30 sec. Hematoxylin was used to stain the nucleus at room temperature for 30 sec. Images were obtained using a digital slide scanner (Pannoramic SCAN, 3DHISTECH). In total, 20 glomeruli randomly selected from the kidney cortex of each section were evaluated.

Primary antibodies were rabbit anti-apelin (cat. no. 11497-1-AP; Proteintech Group, Inc.; 1:200), rabbit anti-APJ (cat. no. ab214369; Abcam; 1:200), rabbit anti-CD31

(cat. no. 77699S; Cell Signaling Technology, Inc.; 1:200), rabbit anti-laminin (cat. no. ARG59198; Arigobio; 1:200), rabbit anti-collagen IV (cat. no. ab236640; Abcam; 1:200).

Masson staining. The sections were deparaffinized and refixed in preheated Bouin's Solution at 56°C for 15 min. After removing the yellow color with running tap water, these sections were stained in Biebrich Scarlet-Acid Fuchsin (cat. no. HT151; MilliporeSigma) for 5 min, phosphotungstic/phosphomolybdic acid Solution for 5 min, Aniline Blue solution for 5 min then dehydrated using an alcohol series. The stained sections were sealed with resinene, then scanned with the digital slide scanner and the blue-colored area represented the fibrotic area. In total, 20 glomeruli randomly selected from the kidney cortex of each section were evaluated.

PicroSirius Red (PSR) staining. The sections were stained in PicroSirius Red staining solution (cat. no. DC0041; Leagene; Beijing Regen Biotechnology Co., Ltd.) at room temperature for 60 min and washed with tap water. Hematoxylin was used to stain the nucleus at room temperature for 30 sec. The stained sections were scanned with digital slide scanner. In total, 20 glomeruli randomly selected from the kidney cortex of each section were evaluated.

Periodic acid-Schiff (PAS) staining. The sections were first stained in PAS oxidant (cat. no. G1281; Beijing Solarbio Science & Technology Co., Ltd.) at room temperature for 5 min and washed with tap water, then stained in Schiff solution for 15 min away from light. Hematoxylin stained the nucleus at room temperature for 1 min. The stained sections were scanned with the digital slide scanner. In total, 20 glomeruli randomly selected from the kidney cortex of each section were evaluated.

Glomerular endothelial cells culture. Native glomerular endothelial cells (GECs) were isolated from the kidneys of APJ^{fl/fl} and APJ^{AEC} mice. Briefly, glomeruli were prepared by sequentially filtration of the cortex of kidneys using mesh sieves with holes of 100, 76 and 54 µm in diameter. The tissues remaining on the mesh sieve with 54 µm holes were collected and digested by type IV collagenase (cat. no. V900893; MilliporeSigma), then transferred to cultural plates and incubated with 20% fetal bovine serum, 1% penicillin/streptomycin in Endothelial Cell Growth Medium (cat. no. 1001; ScienCell Research Laboratories, Inc.) with endothelial cell growth factor for 5 days, which were identified with CD31. When GECs were well-differentiated (~3-5 generations), they were starved for 6-8 h with serum-free Endothelial Cell Medium and then treated with mannitol (25 mmol/l mannitol), HG (25 mmol/l d-glucose) and/or apelin (1.0 nmol/l) for 24 h. Monensin (1.0 µmol/l, cat. no. 1001; CSN11465; CSN Pharma), which prevents protein secretion from the Golgi apparatus, was added 2 h in advance when detecting the expression of secreted proteins.

Transfection of KLF15 small interfering (si)RNA. KLF15 siRNA (si-KLF15) or negative control siRNA (si-NC) were synthesized by Hanheng Biotechnology (Shanghai) Co., Ltd. Cultured GECs with 80% confluency were transfected with

si-KLF15 or si-NC using Lipofectamine® RNAiMAX transfection reagent (cat. no. 1001; 13778075; Invitrogen; Thermo Fisher Scientific, Inc.) at 37°C according to the manufacturer's instructions. After 48 h of transfection, subsequent experiments were performed. The final concentrations of si-KLF15 and its control were 50 nM. The sequences of siRNA were: si-KLF15-1 sense sequence: 5'-CCUGUGAAGGAGGAA CAUTT-3'; si-KLF15-1 antisense sequence: 5'-AAUGUU CCUCCUUCACAGGTT-3'; si-KLF15-3 sense sequence: 5'-CUACCCUGGAGGAGAUUGAAGTT-3'; si-KLF15-3 antisense sequence: 5'-CUUCAUCUCCUCCAGGGUAGTT-3'; si-NC sense sequence: 5'-UUCUCCGAACGUGUCACGUTT-3'; si-NC antisense sequence: 5'-ACGUGACACGUUCGGAGAATT-3'.

Preparation of RNA and reverse transcription-quantitative (RT-q) PCR. Total RNA from cultured GECs was obtained using TRIzol® Reagent (cat. no. 15596026; Thermo Fisher Scientific, Inc.), following the manufacturer's instructions. The concentrations of RNA were measured by detecting the optical density using a microplate reader (Eon; Omega Bio-Tek, Inc.) and the ratio of OD 260 to OD 280 was used to determine purity. Total RNA (1 µg) was reverse-transcribed to the first-strand DNA (cDNA) by using PrimeScript TMRT reagent kit with gDNA eraser (RR047A; Takara Bio, Inc.). The RT-PCR signal was detected by 7500 Real Time PCR System (Applied Biosystems; Thermo Fisher Scientific, Inc.) with a SYBR green qPCR mix (CoWin Biosciences). Pre-denaturation was set at 95°C for 5 min. Denaturation, annealing and extension were completed in 45 cycles at 95°C (15 sec) and 60°C (45 sec) respectively. All reactions were run in triplicate and normalized to the reference gene GAPDH using the 2^{-ΔΔC_q} method (23). Gene-specific primers used to amplify cDNA were: APJ Forward: 5'-TCGTGGTGCTTG TAGTGACC-3'; APJ Reverse: 5'-ATGCAGGTGCAGTAC GGAAA-3'; Laminin-α5 Forward: 5'-AGAGAGCCAGTT CTTGTGCC-3'; Laminin-α5 Reverse: 5'-AAACACTTG GATCGCCTTGC-3'; Laminin-β2 Forward: 5'-GGAGTG ACTGCTAGGTCCGA-3'; Laminin-β2 Reverse: 5'-CTCCAT CCCGACCGTGTG-3'; Collagen IV-α1 Forward: 5'-AAC AACGTCTGCAACTTCGC-3'; Collagen IV-α1 Reverse: 5'-CTTCACAAACCGCACACCTG-3'; KLF15 Forward: 5'-TCAGTGTGACTTTGCTGTCA-3'; KLF15 Reverse: 5'-GGTGGTGGATTCTACACGCA-3'; SIRT3 Forward: 5'-GTCCGGGAGTGTTACAGGTG-3'; SIRT3 Reverse: 5'-ACCATGACCACCACCCTACT-3'; GAPDH Forward: 5'-GGTTGTCTCCTGCGACTTCA-3'; GAPDH Reverse: 5'-GGTGGTCCAGGGTTTCTTACTC-3'.

Western blotting. Cultured GECs were lysed with RIPA lysis buffer (cat. no. R0010; Beijing Solarbio Science & Technology Co., Ltd.) supplemented with protease inhibitor phenylmethanesulfonyl fluoride (PMSF; cat. no. P0100; Beijing Solarbio Science & Technology Co., Ltd.) and centrifuged at 13,500 x g and 4°C for 15 min. Protein concentrations were determined using BCA assay (cat. no. 23227; Thermo Fisher Scientific, Inc.). The proteins from GECs (total 40 µg proteins of each group) were fractionated by electrophoresis on 10% SDS-PAGE and transferred to PVDF membrane (cat. no. IPVH00010; MilliporeSigma). After blocking with 5% skimmed milk at room temperature for 1 h, the PVDF

membranes were incubated with the primary antibody at 4°C overnight followed by an HRP-conjugated secondary antibody at room temperature for 1 h. To verify equal loading, antibody to GAPDH and tubulin were used. The experiment was repeated three times. The results were quantified using ImageJ software (ImageJ 1.48v; National Institutes of Health).

Primary antibodies were rabbit anti-APJ (cat. no. 20341-1-AP; Proteintech Group, Inc.; 1:1,000), rabbit anti-laminin (cat. no. ab233389; Abcam; 1:1,000), rabbit anti-collagen IV (cat. no. E1A0175C; EnoGene; 1:1,000), mouse anti-KLF15 (cat. no. sc-271675; Santa Cruz Biotechnology; 1:1,000), rabbit anti-SIRT3 (cat. no. 5490S; Cell Signaling Technology, Inc.; 1:1,000), rabbit anti-GAPDH (cat. no. 5174S; Cell Signaling Technology, Inc.; 1:2,000), rabbit anti-tubulin (cat. no. 2148S; Cell Signaling Technology, Inc.; 1:2,000), rabbit anti-Histone H3 (cat. no. ab1791; Abcam, 1:2,000). Secondary antibodies were donkey anti-mouse IgG (cat. no. SA00001-8; Proteintech Group, Inc.; 1:2,000), donkey anti-rabbit IgG-HRP (cat. no. 7074S, Cell Signaling Technology, Inc.; 1:2,000).

Mitochondrial extraction of GECs. Cultured GECs were collected and centrifuged (800 x g) for 5 min at 4°C according to the instructions of the Mitochondrial Extraction Kit (cat. no. BA62; EnoGene). The supernatant obtained by centrifugation was added along the tube wall into a tube containing solution A and centrifuged (15,000 x g) for 10 min at 4°C. The sediments, mitochondria, were then rinsed and resuspended with storage solution for preservation.

SIRT3 activity detection. According to the manufacturer's instructions for the Epigenase Universal SIRT Activity/Inhibition Assay Kit (cat. no. P-4036; EpiGentek), prepared working buffer, solution and mitochondria extracted from treated GECs were added to the corresponding wells, including blank wells, no NAD control (NNC) wells, standard wells and sample wells. The plate was incubated at 37°C for 90 min and antibody binding and signal enhancing performed. Then, to each well was added 100 µl of developer solution and incubated at room temperature for 10 min away from light. After the color in the positive control wells turned medium blue, 100 µl of stop solution was added to each well to stop enzyme reaction and the absorbance was read on a microplate reader (Eon; Omega Bio-Tek, Inc.) within 2-10 min at 450 nm with an optional reference wavelength of 655 nm. The formula of calculating SIRT3 activity was:

$$\text{SIRT Activity (OD/min/mg)} = \frac{(\text{Sample OD} - \text{NNC OD})}{(\text{Protein Amount}(\mu\text{g}) \times \text{incubation time})} \times 1,000$$

Separation of nuclear and cytoplasmic fractions. The separation was performed according to the instructions with Minute Cytoplasmic and Nuclear Extraction Kit (cat. no. SC-003; Invent Biotechnologies, Inc.) and analyzed using western blotting. 3-TYP (cat. no. S8628; Selleck Chemicals) with a final concentration of 20 nM was used to inhibit SIRT3 activity in GECs. Briefly, cultured GECs were collected in 150 µl cytoplasmic extraction buffer. Cytoplasmic proteins were obtained with centrifugation (16,000 x g) for 5 min at 4°C. The precipitates were resuspended using 75 µl nuclear extraction buffer, then centrifuged 16,000 x g at 4°C for 30 sec to separate nuclear proteins.

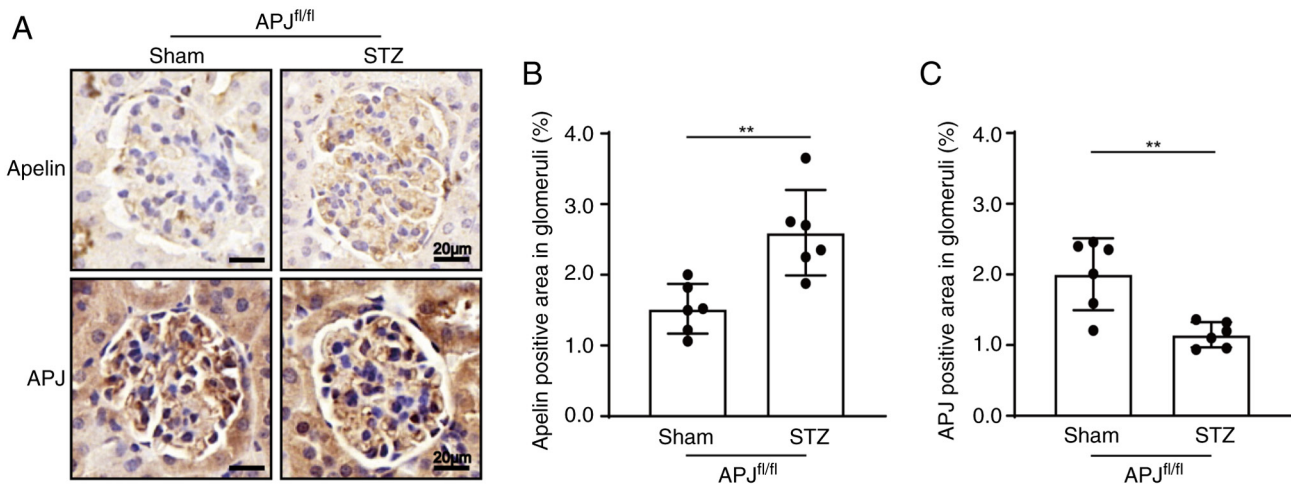


Figure 1. Diabetes increases the expression of apelin and decreased the expression of APJ in glomeruli. (A) Representative images of immunohistochemistry staining for apelin and APJ in glomerulus of APJ^{fl/fl} mice. The target protein was shown as brown. Scale bar, 20 μm. (B) Quantitative data of apelin in glomeruli (n=6). (C) Quantitative data of APJ in glomeruli (n=6). The data are presented as the mean ± SEM. **P<0.01. APJ, apelin/apelin receptor; STZ, streptozotocin.

Statistical analysis. The data were analyzed using SPSS version 25.0 for the PC (IBM Corp.). All data were normally distributed according to the Shapiro-Wilk test and presented as mean ± standard error of the mean. Differences were evaluated for significance using the unpaired t-test for two groups or one-way ANOVA for more than two groups, which followed by Tukey's post hoc test. The variance homogeneity was evaluated using Levene's tests. All reported P-values were two-tailed. P<0.05 was considered to indicate a statistically significant difference.

Results

Diabetes increases the expression of apelin and decreased the expression of APJ in glomeruli. The results of immunohistochemistry showed that the expression of apelin in glomeruli increased from 1.52±0.14% to 2.60±0.25% in diabetic mice (n=6; P<0.01; Fig. 1A and B). However, the expression of APJ in glomeruli decreased from 2.00±0.21% to 1.15±0.07% in diabetic mice (n=6; P<0.01, Fig. 1A and C).

Apelin decreases the random blood glucose level in diabetic mice. Compared with control mice, the random blood glucose was significantly increased from 10.57±0.28 mmol/l to 18.73±0.87 mmol/l in diabetic mice (n=6; P<0.01), which reversed to 12.70±0.86 mmol/l by apelin infusion (n=6; P<0.05; Table SI). These phenomena were partly amplified following APJ knockout in endothelial cells whose APJ expression in glomerular endothelial cells decreased from 2.00±0.21% in APJ^{fl/fl} mice to 0.34±0.06% in APJ^{ΔEC} mice (n=6; P<0.001, Fig. S1), which showed that random blood glucose increased from 9.48±0.29 mmol/l to 27.05±1.69 mmol/l in diabetic mice and reversed to 18.83±1.47 mmol/l by apelin infusion (n=6; P<0.05; Table SI).

Apelin improves renal function in diabetic mice. Urine output (increased from 0.93±0.16 to 4.87±0.99 ml/24 h) and urine protein content (increased from 1.04±0.16 to 16.84±2.70 mg/24 h) were both increased in diabetic

APJ^{fl/fl} mice (n=6; P<0.05) and decreased following apelin treatment (urine output: 2.04±0.42 ml/24 h, urine protein: 5.97±0.84 mg/24 h, n=6; P<0.05; Table SI). Meanwhile, compared with control mice, serum creatinine (SCR) was also significantly increased in diabetic APJ^{fl/fl} mice (increased from 10.54±1.80 to 25.38±4.48 μmol/l), which was decreased by apelin to 13.60±1.55 μmol/l (n=6; P<0.05; Table SI).

However, apelin did not show similar effects on urine output, urine protein and SCR in diabetic APJ^{ΔEC} mice. The urine output increased from 1.03±0.21 to 4.24±1.43 ml/24 h in diabetic APJ^{ΔEC} mice (n=6; P<0.01), which changed to 3.25±0.60 ml/24 h following apelin infusion (n=6; P>0.05; Table SI). The urine protein increased from 1.53±0.35 to 13.09±6.92 mg/24 h in diabetic APJ^{ΔEC} mice (n=6; P<0.01), which changed to 7.80±1.58 mg/24 h following apelin infusion (n=6; P>0.05; Table SI). The SCR increased from 9.25±1.95 to 21.08±3.10 μmol/l in diabetic APJ^{ΔEC} mice (n=6; P<0.01), which changed to 16.32±1.95 μmol/l following apelin infusion (n=6; P>0.05; Table SI).

Apelin reduces GBM thickening and glomerular fibrosis in diabetic mice dependent on endothelial APJ. PAS staining showed that compared with control mice, matrix deposition increased in diabetic mice both in APJ^{fl/fl} mice (from 9.73±0.42% to 14.60±0.76%, n=6; P<0.001) and APJ^{ΔEC} mice (from 10.24±0.26% to 14.38±0.94%, n=6; P<0.001), which was reversed by apelin to 10.76±0.34% in diabetic APJ^{fl/fl} mice (n=6; P<0.001), but not in apelin treated diabetic APJ^{ΔEC} mice (12.75±0.70%, n=6; P>0.05, Fig. 2A and B).

Masson staining showed that compared with control mice, the fibrotic area of glomeruli was significantly increased both in diabetic APJ^{fl/fl} mice (from 2.71±0.22% to 7.42±0.33%, n=6; P<0.001) and diabetic APJ^{ΔEC} mice (from 2.45±0.17% to 7.89±0.37%, n=6; P<0.001), which was reversed by apelin to 5.32±0.21% in diabetic APJ^{fl/fl} mice (n=6; P<0.001), but not in apelin treated diabetic APJ^{ΔEC} mice (6.92±0.36%, n=6; P>0.05, Fig. 2A and C).

PSR staining showed that compared with control mice, the amount of collagen fiber was also increased both in diabetic APJ^{fl/fl} mice (from 2.24±0.11% to 5.17±0.21%, n=6; P<0.001)

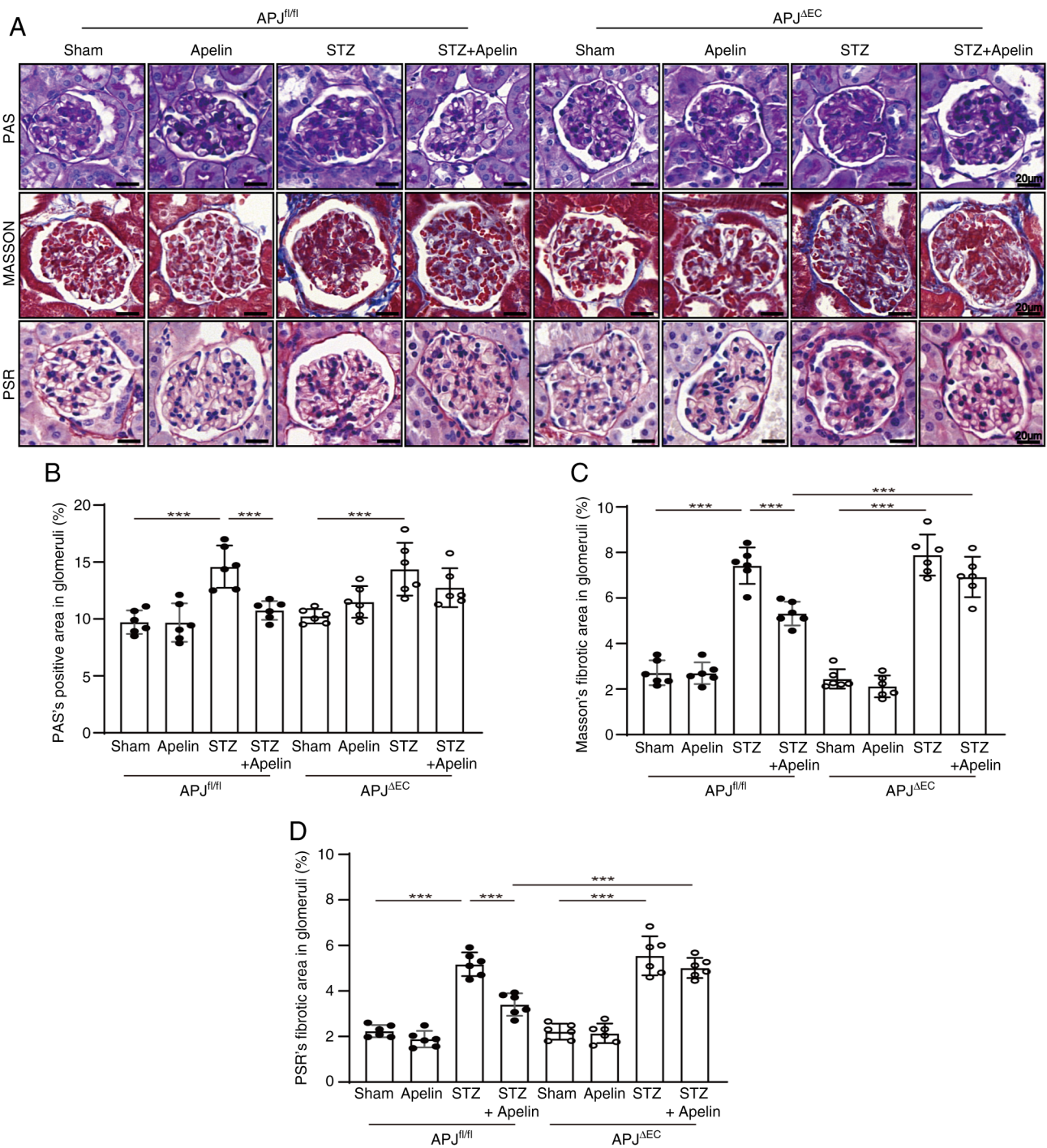


Figure 2. Apelin reduces GBM thickening and glomerular fibrosis in diabetic mice dependent on endothelial APJ. (A) Representative images of PAS, Masson and PSR staining for glomerulus in each group. Scale bar, 20 μ m. (B) Quantitative data of PAS staining (n=6). (C) Quantitative data of PSR staining (n=6). (D) Quantitative data of Masson staining (n=6). The data are presented as the mean \pm SEM. Solid dots represent APJ^{fl/fl} mice and open dots represent APJ^{ΔEC} mice. ***P<0.001. GBM, glomerular basement membrane; APJ, apelin/apelin receptor; PAS, Periodic acid-Schiff; PSR, PicroSirius Red; STZ, streptozotocin.

and diabetic APJ^{ΔEC} mice (from 2.21 \pm 0.14% to 5.54 \pm 0.35%, n=6; P<0.001), which was reversed by apelin to 3.41 \pm 0.20% in diabetic APJ^{fl/fl} mice (n=6; P<0.001), but not in apelin treated diabetic APJ^{ΔEC} mice (5.01 \pm 0.18%, n=6; P>0.05, Fig. 2A and D).

Apelin decreases the expression of laminin and collagen IV in glomeruli dependent on endothelial APJ. To confirm the effects of apelin on the expression of the GBM components, immunohistochemistry for laminin and collagen IV was

performed. The results showed that the positive area of laminin in glomeruli was significantly increased in diabetic mice (from 3.13 \pm 0.26% in APJ^{fl/fl} mice to 7.04 \pm 0.26% in diabetic APJ^{fl/fl} mice, n=6; P<0.001) but was reversed by apelin to 3.57 \pm 0.18% (n=6; P<0.001, Fig. 3A and B). Notably, the expression of laminin was also increased from 2.70 \pm 0.20% in APJ^{ΔEC} to 6.10 \pm 0.48% in diabetic APJ^{ΔEC} mice (n=6; P<0.001), which was decreased to 5.27 \pm 0.26% by apelin in diabetic APJ^{ΔEC} mice (n=6; P>0.05; Fig. 3A and B).

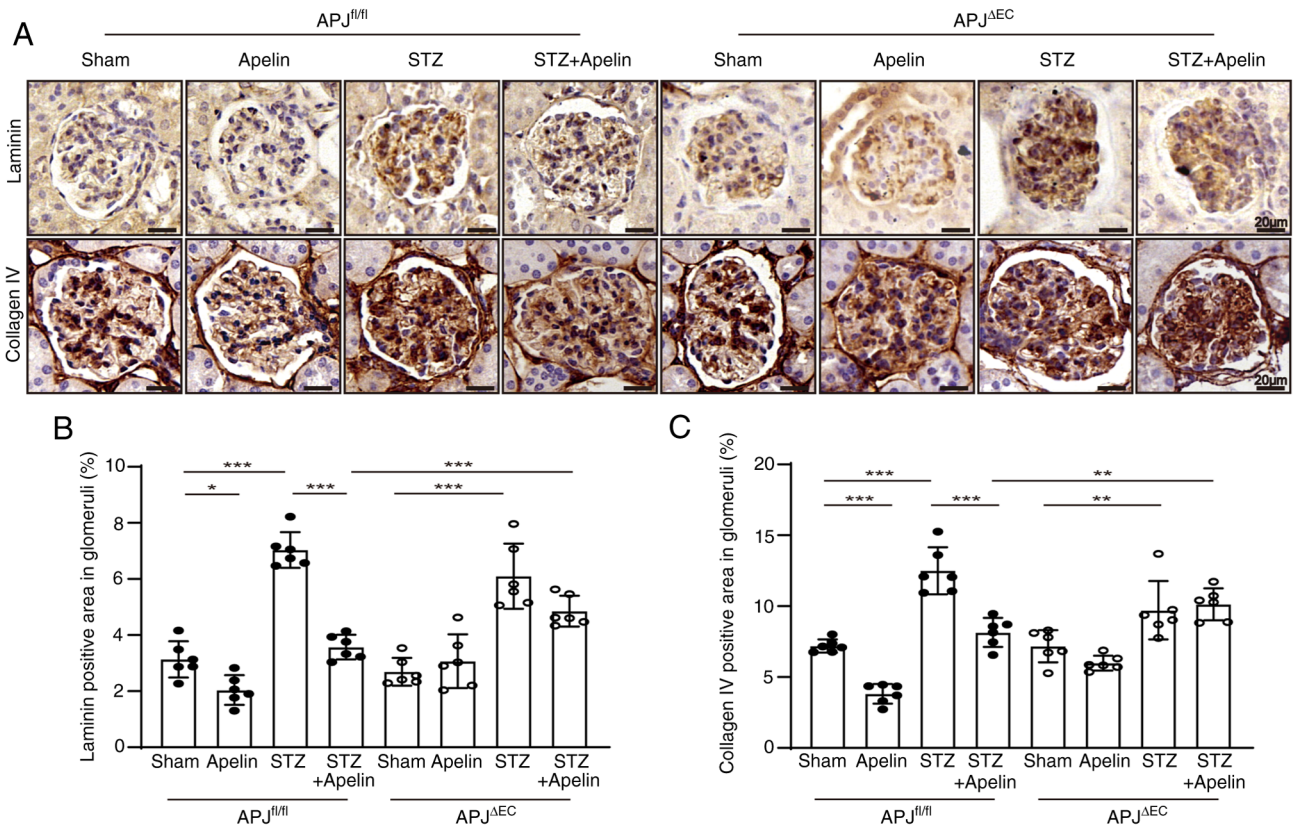


Figure 3. Apelin decreases the expression of laminin and collagen IV in glomeruli dependent on endothelial APJ. (A) Representative images of immunohistochemistry staining for laminin and collagen IV in glomerulus of each group. The target protein is shown as brown. Scale bar, 20 μ m. (B) Quantitative data of laminin in glomerulus (n=6). (C) Quantitative data of collagen IV in glomerulus (n=6). The data are presented as the mean \pm SEM. Solid dots represent APJ^{fl/fl} mice and open dots represent APJ^{ΔEC} mice. *P<0.05, **P<0.01, ***P<0.001. APJ, apelin/apelin receptor; STZ, streptozotocin.

Similar results were obtained for collagen IV immunostaining. The positive area in glomeruli was increased from $7.19 \pm 0.19\%$ in APJ^{fl/fl} mice to $12.50 \pm 0.67\%$ in diabetic APJ^{fl/fl} mice and reversed by apelin to $8.15 \pm 0.42\%$ in diabetic APJ^{fl/fl} mice (n=6; P<0.001, Fig. 3A and C). However, the positive area of collagen IV increased from $7.17 \pm 0.46\%$ in APJ^{ΔEC} to $9.71 \pm 0.84\%$ in diabetic APJ^{ΔEC} mice (n=6; P<0.01), which was variated to $10.14 \pm 0.46\%$ in apelin treated diabetic APJ^{ΔEC} mice (n=6; P>0.05, Fig. 3A and C).

Apelin inhibits the synthesis of laminin and collagen IV in GECs dependent on APJ. To fully understand the effects of apelin on GECs, primary glomerular endothelial cells (GECs) from APJ^{fl/fl} mice and APJ^{ΔEC} mice were extracted. The results showed that APJ mRNA and protein were both decreased in GECs following APJ knockout (0.61 ± 0.05 fold of mRNA and 0.79 ± 0.01 fold of protein, n=3; P<0.01, Fig. S2).

It had been reported that the isoforms provided by endothelial cells in GBM are laminin $\alpha 5\beta 2\gamma 1$ (laminin 521) and collagen IV $\alpha 1\alpha 2\alpha 1$ (3,7,8), therefore expression of laminin- $\alpha 5$, laminin- $\beta 2$ and collagen IV- $\alpha 1$ were detected. The results showed that apelin decreased the mRNA of laminin- $\alpha 5$ (0.20 ± 0.09 fold, n=3; P<0.01), laminin- $\beta 2$ (0.13 ± 0.05 folds; n=3; P<0.01) and collagen IV- $\alpha 1$ (0.35 ± 0.12 folds; n=3; P<0.01) in mannitol cultured GECs (Fig. 4A), but not following APJ knockout (1.28 ± 0.13 fold of laminin- $\alpha 5$ mRNA, 1.41 ± 0.16 fold of laminin- $\beta 2$ mRNA, 1.06 ± 0.13 fold of collagen IV- $\alpha 1$ mRNA, n=3; P>0.05; Fig. 4B). Similarly, apelin also decreased

the mRNA of laminin- $\alpha 5$ (from 1.34 ± 0.17 fold to 0.37 ± 0.10 folds), laminin- $\beta 2$ (from 1.49 ± 0.29 fold to 0.44 ± 0.09 folds) and collagen IV- $\alpha 1$ (from 1.05 ± 0.03 fold to 0.51 ± 0.08 folds) in high glucose cultured GECs (n=3; P<0.01, Fig. 4A), but not in GECs from APJ^{ΔEC} mice (from 1.22 ± 0.13 fold of laminin- $\alpha 5$ mRNA, from 1.51 ± 0.12 fold to 1.95 ± 0.18 fold of laminin- $\beta 2$ mRNA, from 0.89 ± 0.08 fold to 0.98 ± 0.15 fold of collagen IV- $\alpha 1$ mRNA, n=3; P>0.05, Fig. 4B).

In order to confirm the effects of apelin/APJ on ECM synthesis in GECs, protein expression of laminin and collagen IV were detected after inhibiting the secretion of proteins by destroying Golgi apparatus with monensin. The results showed that apelin reduced both laminin (from 1.21 ± 0.03 fold to 0.96 ± 0.02 fold, n=3; P<0.05; Fig. 4C and D) and collagen IV (from 1.06 ± 0.06 fold to 0.69 ± 0.08 fold, n=3; P<0.05; Fig. 4C and E) under high glucose condition, which was cancelled following APJ knockout (laminin from 1.19 ± 0.16 fold to 1.09 ± 0.09 fold, collagen IV from 1.21 ± 0.10 fold to 1.11 ± 0.09 fold, n=3; P>0.05, Fig. 4F-H).

KLF15 mediates the effects of apelin/APJ in GECs. The results from western blotting showed that apelin increased expression of KLF15 (from 0.59 ± 0.05 fold to 0.80 ± 0.05 fold, n=3; P<0.05; Fig. 5A and B) under high glucose condition. The results also showed that the silenced KLF15 (from 0.86 ± 0.02 fold to 0.39 ± 0.16 fold of KLF15 mRNA, from 0.95 ± 0.04 fold to 0.59 ± 0.09 fold of KLF15 protein by using si-KLF15-3, n=3; P<0.01; Figs. 5C and S3) upregulated the decreasing effects

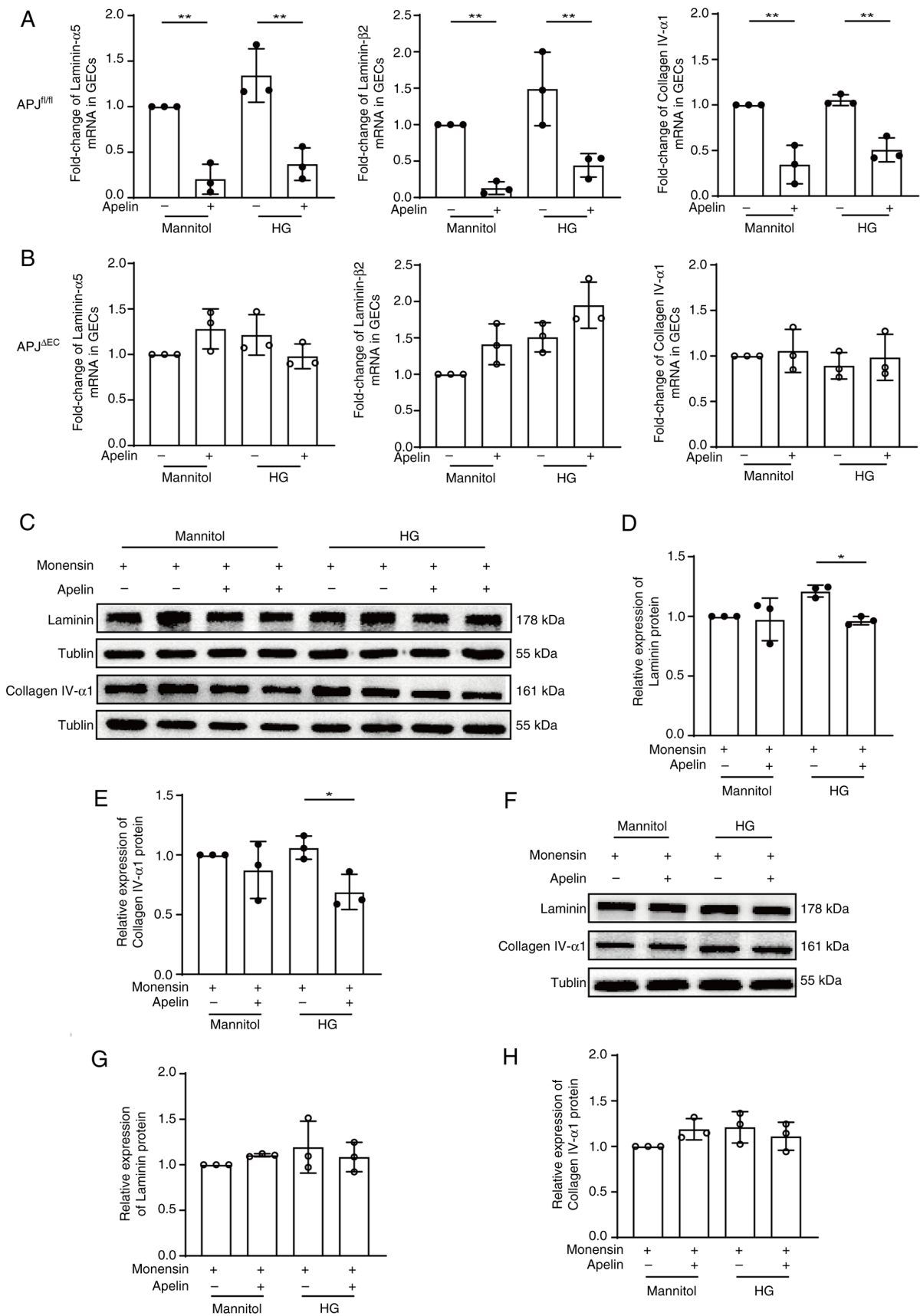


Figure 4. Apelin inhibited the synthesis of laminin and collagen IV in GECs dependent on APJ. (A) Quantitative analysis of reverse transcription-quantitative PCR results for laminin- α 5, laminin- β 2 and collagen IV- α 1 in GECs of APJ^{fl/fl} mice (n=3). (B) Quantitative analysis of reverse transcription-quantitative PCR results for laminin- α 5, laminin- β 2 and collagen IV- α 1 in GECs of APJ^{ΔEC} mice (n=3). (C) Representative images of western blotting for laminin and collagen IV in GECs of APJ^{fl/fl} mice. (D) Quantitative analysis of western blotting for laminin (n=3). (E) Quantitative analysis of western blotting for collagen IV (n=3). (F) Representative images of western blotting for laminin and collagen IV in GECs of APJ^{ΔEC} mice. (G) Quantitative analysis of western blotting for laminin (n=3). (H) Quantitative analysis of western blotting for collagen IV (n=3). The data are presented as the mean \pm SEM. Solid dots represent APJ^{fl/fl} mice and open dots represent APJ^{ΔEC} mice. *P<0.05, **P<0.01. GECs, glomerular endothelial cells; APJ, apelin/apelin receptor; HG, 25 mM d-glucose.

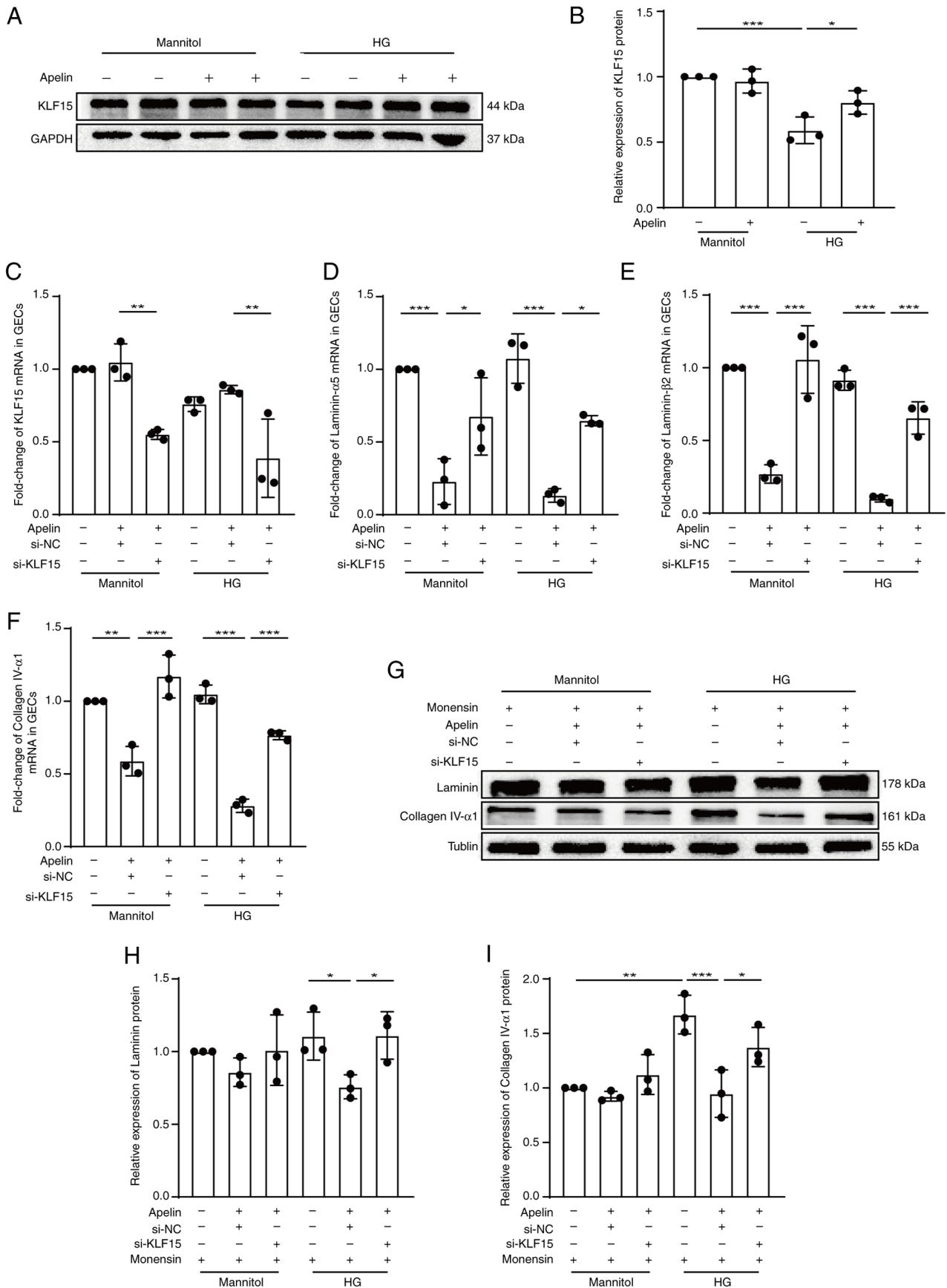


Figure 5. KLF15 mediates the effects of apelin/APJ in GECs. (A) Representative images of western blotting for KLF15 in GECs of APJ^{fl/fl} mice. (B) Quantitative analysis of western blotting for KLF15 (n=3). Quantitative analysis of RT-qPCR results for (C) KLF15, (D) laminin- α 5, (E) laminin- β 2 and (F) collagen IV- α 1 in APJ^{fl/fl} mice (n=3). (G) Representative images of western blotting for laminin and collagen IV in GECs of APJ^{fl/fl} mice. (H) Quantitative analysis of western blotting for laminin (n=3). (I) Quantitative analysis of western blotting for collagen IV (n=3). The data are presented as the mean \pm SEM. *P<0.05, **P<0.01, ***P<0.001. KLF15, Krüppel-like factor 15; APJ, apelin/apelin receptor; GECs, glomerular endothelial cells; RT-qPCR, reverse transcription-quantitative PCR; HG, 25 mM d-glucose.

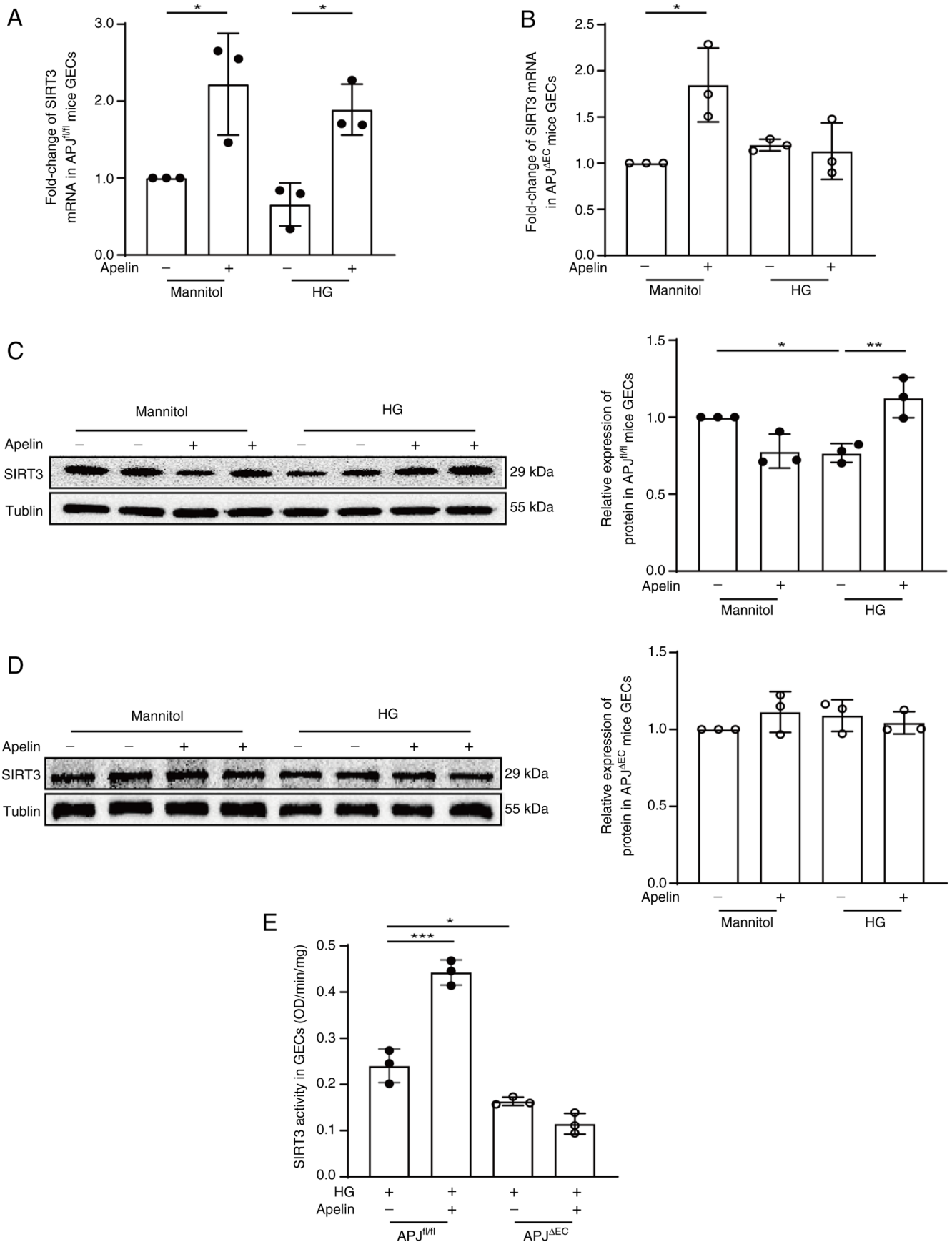


Figure 6. Apelin/APJ increased the expression and activity of SIRT3. (A) Quantitative analysis of RT-qPCR results for SIRT3 in GECs of APJ^{fl/fl} mice (n=3). (B) Quantitative analysis of RT-qPCR results for SIRT3 in GECs of APJ^{ΔEC} mice (n=3). (C) Representative images and quantitative analysis of western blotting for SIRT3 in GECs of APJ^{fl/fl} mice (n=3). (D) Representative images and quantitative analysis of western blotting for SIRT3 in GECs of APJ^{ΔEC} mice (n=3). (E) Quantitative analysis for SIRT3 activity in GECs of APJ^{fl/fl} mice. The data are presented as the mean ± SEM. Solid dots represent APJ^{fl/fl} mice and open dots represent APJ^{ΔEC} mice. *P<0.05, **P<0.01, ***P<0.001. APJ, apelin/apelin receptor; SIRT3, sirtuin-3; RT-qPCR, reverse transcription-quantitative PCR; GECs, glomerular endothelial cells; HG, 25 mM d-glucose.

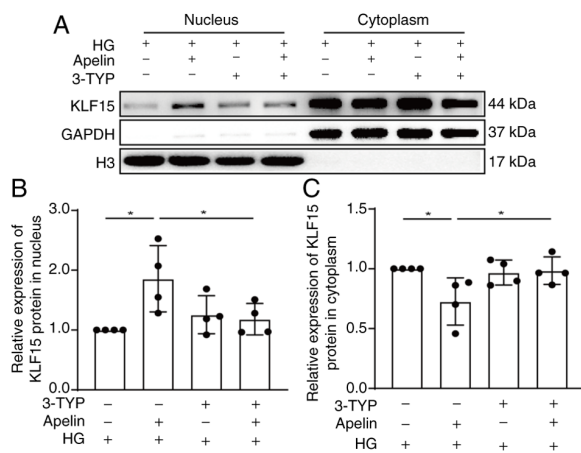


Figure 7. Apelin/APJ promotes deacetylation and translocation of KLF15 via SIRT3. (A) Representative images of western blotting for KLF15 nucleocytoplasmic separation in GECs of APJ^{fl/fl} mice. (B) Quantitative analysis of western blotting for KLF15 in nucleus (n=4). (C) Quantitative analysis of western blotting for KLF15 in cytoplasm (n=4). The data are presented as the mean \pm SEM. *P<0.05. APJ, apelin/apelin receptor; KLF15, Krüppel-like factor 15; SIRT3, sirtuin-3; GECs, glomerular endothelial cells; HG, 25 mM d-glucose.

of apelin on mRNA (from 0.13 ± 0.03 fold to 0.65 ± 0.02 fold of laminin- $\alpha 5$ mRNA, from 0.10 ± 0.01 fold to 0.65 ± 0.06 fold of laminin- $\beta 2$ mRNA, from 0.28 ± 0.03 fold to 0.77 ± 0.02 fold of collagen IV- $\alpha 1$ mRNA, n=3; P<0.05; Fig. 5D-F) and protein (laminin from 0.76 ± 0.05 fold to 1.11 ± 0.09 fold, collagen IV from 0.95 ± 0.13 fold to 1.38 ± 0.10 fold, n=3; P<0.05, Fig. 5G-I) of laminin and collagen IV under high glucose condition in GECs.

SIRT3 mediates the effects of apelin/APJ on KLF15 in GECs. Transcriptional activity of KLF15 is regulated by SIRT3 (20). Therefore, the effects of apelin on the expression and activity of SIRT3 in GECs were detected. The results showed that apelin increased SIRT3 mRNA expression from 0.66 ± 0.16 fold to 1.89 ± 0.19 fold under high glucose condition, which was reversed to 1.13 ± 0.18 fold following APJ knockout (n=3; P<0.05; Fig. 6A and B). The results from western blotting showed that apelin increased the expression of SIRT3 protein from 0.77 ± 0.04 fold to 1.13 ± 0.08 fold (n=3; P<0.01, Fig. 6C) under high glucose conditions, which were cancelled (from 1.09 ± 0.06 fold to 1.04 ± 0.04 fold; n=3; P>0.05; Fig. 6D) following APJ knockout in GECs. Meanwhile, the activity of SIRT3 was also significantly increased by apelin in GECs under high glucose condition (from 0.24 ± 0.02 to 0.44 ± 0.02 OD/min/mg; n=3; P<0.001), which were cancelled following APJ knockout (from 0.16 ± 0.00 to 0.11 ± 0.01 OD/min/mg; n=3; P>0.05; Fig. 6E).

To verify apelin promoted deacetylation and translocation of KLF15 to nucleus via SIRT3, SIRT3 activity was inhibited with 3-TYP. The results showed that 3-TYP significantly reversed the increasing effects of apelin on the translocation of KLF15 into nucleus (from 1.86 ± 0.28 fold to 1.18 ± 0.13 fold; n=4; P<0.05; Fig. 7A and B) under high glucose conditions.

Discussion

The present study revealed for the first time, to the best of the authors' knowledge, that apelin may relieve GBM thickening

in DM via endothelial APJ activated SIRT3-KLF15 pathway. Apelin reduced glomerular fibrosis and GBM thickening by decreasing laminin and collagen IV expression via the promotion of KLF15 translocation into nucleus, which was dependent on APJ-activated SIRT3 in GECs under high glucose conditions.

GBM thickening is the earliest morphological change of DN and is followed by glomerulosclerosis accompanied by progressive renal dysfunction (2,3,8,24). Importantly, GBM thickening is reportedly associated with GECs dysfunction (6-8). On the basis of reports that apelin/APJ improves endothelial dysfunction in DM (15,16), the effects of apelin on glomerular morphological defect were evaluated in diabetic mice. Consistent with previous reports (25,26), increased apelin (Fig. 1) alleviated glomerular fibrosis and GBM thickening (Fig. 2) under diabetic conditions. Did these effects of apelin depend on its endothelial receptor, APJ?

Endothelial-specific APJ knockout mice were then generated to investigate whether APJ mediated the effects of apelin on endothelial cells during DN. APJ knockout partly cancelled the protective effects of apelin on renal damages in DN (Fig. 2 and Table SI), which indicated that apelin may regulate endothelial functions by combining with APJ. The next question was: What happens after apelin combines with APJ during GBM thickening under diabetic conditions?

One of the causes of GBM thickening is increased ECM synthesis in GECs, which leads to protein accumulation in GBM (4,27). It has been reported that the major components of GBM include laminin, collagen IV, nidogens and heparan sulfate proteoglycans (3). Nidogens and heparan sulfate proteoglycans not only express marginally, but also have little effect on GBM function. Therefore, the expression of laminin and collagen IV, the two most abundant components of the GBM, were detected (3,10,28,29) after apelin/APJ were artificially altered in mice. Apelin treatment reversed both the laminin and collagen IV content in glomeruli in diabetic mice (Fig. 3). These findings suggested that apelin may reduce GBM thickening by decreasing the deposition of laminin and collagen IV in glomeruli. Furthermore, APJ knockout in GECs partly cancelled the effects of apelin on laminin and collagen IV in glomeruli (Fig. 3). Together, these results suggested that apelin alleviated GBM thickening by decreasing laminin and collagen IV expression in GECs via combination with endothelial APJ. It was therefore asked: What are the intracellular mechanisms for apelin/APJ in regulating the ECM synthesis and deposition?

Transcription and translation might both be involved in ECM synthesis in GECs (4,17), therefore mRNA and protein levels of laminin 521 and collagen IV $\alpha 1\alpha 2\alpha 1$ were detected in cultured GECs. mRNA and protein levels of laminin and collagen IV in GECs were both decreased by apelin (Fig. 4). As these two proteins are specific isoforms in the GBM that are expressed by GECs (3,7,8), these results suggested that apelin might alleviate GBM thickening by inhibiting the transcription and translation of GBM proteins in GECs during DM. Notably, the present study also noted that mannitol almost completely simulated the effects of hyperglycemia on mRNA levels of GBM proteins in GECs (Fig. S4), which suggested that osmolarity might be the key factor for hyperglycemia to increase ECM expression in GECs. As APJ was reported to mediate

mechanical stimuli in cells (30), is it possible that apelin decreases GBM protein synthesis in GECs by counteracting hyperglycemia or hypertonic induced dysfunction in GECs?

KLF15, a transcription factor that reportedly inhibits ECM synthesis and fibrosis (21,22), was increased by apelin in GECs under hyperglycemia conditions (Fig. 5A and B). Furthermore, the effects of apelin on laminin and collagen IV were cancelled following KLF15 silencing (Fig. 5D-I). KLF15 was therefore hypothesized to be the key intracellular signaling molecule by which apelin regulates ECM synthesis in GECs.

KLF15 activity is regulated by SIRT3-induced deacetylation (20), which is also downstream of apelin (18,19). In the present study, apelin increased both expression and activity of SIRT3 in GECs and these effects disappeared following APJ knockout (Fig. 6). These results indicated that apelin activates SIRT3 pathway in an APJ-dependent manner. The present study also demonstrated that the effect of apelin on promoting KLF15 translocation into nucleus was reduced after inhibiting SIRT3 activity (Fig. 7). These findings confirmed that apelin promotes KLF15 deacetylation and translocation into the nucleus by increasing SIRT3 expression and activity. Moreover, they also prove for the first time, to the best of the authors' knowledge, that the SIRT3-KLF15 pathway regulated the transcription of ECM in GECs, which may have a protective role in DN.

However, it must be noted that apelin infusion also decreased hyperglycemia, which is the most important risk factor for GECs dysfunction during DM (31-33). In the present study, apelin decreased the random blood glucose levels in diabetic mice both with and without APJ knockout (Table SI), suggesting that apelin may alleviate DN by decreasing blood glucose in a manner independent of endothelial APJ. Notably, APJ had a stronger hypoglycemic effect than apelin in diabetic mice, which might be related to β -arrestin signaling (34) activated by hypertonic or mechanical stimuli (30). However, high glucose did not change APJ expression in GECs in the present study (Fig. S5) despite decreased APJ in the glomeruli of diabetic mice (Fig. 1). These results suggested that APJ, but not apelin, reduced blood glucose in diabetic mice. It may therefore be concluded that apelin exerts anti-diabetic nephropathic effects via endothelial APJ and relevant downstream molecules, rather than by controlling blood glucose. However, the limitation of the present study is that it was unable to elucidate how apelin might reduce blood glucose by affecting other renal cells.

In summary, the current study demonstrated for the first time, to the best of the authors' knowledge, that apelin reduced GBM thickening by preventing GECs from synthesizing laminin and type IV collagen, which were dependent on endothelial APJ activated SIRT3-KLF15 pathway. Although apelin/APJ has diverse roles in diabetic nephropathy, the present findings indicated the protective effect of apelin/APJ, which might provide a potential therapeutic target for DN.

Acknowledgements

Not applicable.

Funding

The present study was supported by the National Natural Science Foundation of China (grant no. 32071112) and the

Science and Technology Program of the Beijing Municipal Education Commission (grant no. KM201910025028).

Availability of data and materials

The data generated in the present study may be requested from the corresponding author.

Authors' contributions

MH, JY and XZ designed the research. MH, JC and YL performed the experiments. MH analyzed the data. JY, MH and XZ wrote the manuscript and were responsible for making revisions. XZ secured funding. MH and XZ confirmed the authenticity of all the raw data. All authors read and approved the final manuscript.

Ethics approval and consent to participate

All the animal experiments were approved by the Ethics Committee for Animal Experiments of Capital Medical University (approval no. AEEI-2020-045) and according to the Guide for the Care and Use of Laboratory Animals (National Institutes of Health).

Patient consent for publication

Not applicable.

Competing interests

The authors declare that they have no competing interests.

References

- Papadopoulou-Marketou N, Chrousos GP and Kanaka-Gantenbein C: Diabetic nephropathy in type 1 diabetes: A review of early natural history, pathogenesis, and diagnosis. *Diabetes Metab Res Rev* 33: 2841, 2017.
- Alicic RZ, Rooney MT and Tuttle KR: Diabetic kidney disease: Challenges, progress, and possibilities. *Clin J Am Soc Nephrol* 7: 2032-2045, 2017.
- Naylor RW, Morais MRPT and Lennon R: Complexities of the glomerular basement membrane. *Nat Rev Nephrol* 17: 112-127, 2021.
- Marshall CB: Rethinking glomerular basement membrane thickening in diabetic nephropathy: Adaptive or pathogenic? *Am J Physiol Renal Physiol* 311: F831-F843, 2016.
- Tuleta I and Frangogiannis NG: Diabetic fibrosis. *Biochim Biophys Acta Mol Basis* 1867: 166044, 2021.
- Petrazzuolo A, Sabiu G, Assi E, Maestroni A, Pastore I, Lunati ME, Montefusco L, Loretelli C, Rossi G, Ben Nasr M, *et al*: Broadening horizons in mechanisms, management, and treatment of diabetic kidney disease. *Pharmacol Res* 190: 106710, 2021.
- St John PL and Abrahamson DR: Glomerular endothelial cells and podocytes jointly synthesize laminin-1 and -11 chains. *Kidney Int* 60: 1037-1046, 2001.
- Kriz W, Löwen J, Federico G, van den Born J, Gröne E and Gröne HJ: Accumulation of worn-out GBM material substantially contributes to mesangial matrix expansion in diabetic nephropathy. *Am J Physiol Renal Physiol* 312: F1101-F1111, 2017.
- Stefan G, Stancu S, Zugravu A, Petre N, Mandache E and Mircescu G: Histologic predictors of renal outcome in diabetic nephropathy: Beyond renal pathology society classification. *Medicine (Baltimore)* 98: e16333, 2019.
- Lenoir O, Jasiek M, Hénique C, Guyonnet L, Hartleben B, Bork T, Chipont A, Flosseau K, Bensaada I, Schmitt A, *et al*: Endothelial cell and podocyte autophagy synergistically protect from diabetes-induced glomerulosclerosis. *Autophagy* 11: 1130-1145, 2015.

11. Wardle EN: How does hyperglycaemia predispose to diabetic nephropathy? *QJM* 89: 943-951, 1996.
12. DeFronzo RA, Reeves WB and Awad AS: Pathophysiology of diabetic kidney disease: impact of SGLT2 inhibitors. *Nat Rev Nephrol* 17: 319-334, 2021.
13. Eringa EC, Serne EH, Meijer RI, Schalkwijk CG, Houben AJ, Stehouwer CD, Smulders YM and van Hinsbergh VW: Endothelial dysfunction in (pre) diabetes: Characteristics, causative mechanisms and pathogenic role in type 2 diabetes. *Rev Endocr Metab Disord* 14: 39-48, 2013.
14. El Husseny MW, Mamdouh M, Shaban S, Ibrahim Abushouk A, Zaki MM, Ahmed OM and Abdel-Daim MM: Adipokines: Potential therapeutic targets for vascular dysfunction in type II Diabetes mellitus and obesity. *J Diabetes Res* 2017: 8095926, 2017.
15. Kim S, Kim S, Hwang AR, Choi HC, Lee JY and Woo CH: Apelin-13 inhibits methylglyoxal-induced unfolded protein responses and endothelial dysfunction via regulating AMPK pathway. *Int J Mol Sci* 21: 4069, 2020.
16. Cheng J, Luo X, Huang Z and Chen L: Apelin/APJ system: A potential therapeutic target for endothelial dysfunction-related diseases. *J Cell Physiol* 234: 12149-12160, 2019.
17. Mariappan MM: Signaling mechanisms in the regulation of renal matrix metabolism in diabetes. *Exp Diabetes Res* 2012: 749812, 2012.
18. Ni T, Lin N, Huang X, Lu W, Sun Z, Zhang J, Lin H, Chi J and Guo H: Icarin ameliorates diabetic cardiomyopathy through apelin/sirt3 signalling to improve mitochondrial dysfunction. *Front Pharmacol* 11: 256, 2020.
19. Guan YM, Diao ZL, Huang HD, Zheng JF, Zhang QD, Wang LY and Liu WH: Bioactive peptide apelin rescues acute kidney injury by protecting the function of renal tubular mitochondria. *Amino Acids* 53: 1229-1240, 2021.
20. Li N, Zhang J, Yan X, Zhang C, Liu H, Shan X, Li J, Yang Y, Huang C, Zhang P, *et al*: SIRT3-KLF15 signaling ameliorates kidney injury induced by hypertension. *Oncotarget* 8: 39592-39604, 2017.
21. Rane MJ, Zhao Y and Cai L: Krüppel-like factors (KLFs) in renal physiology and disease. *EBioMedicine* 40: 743-750, 2019.
22. Gao X, Huang L, Grosjean F, Esposito V, Wu J, Fu L, Hu H, Tan J, He C, Gray S, *et al*: Low-protein diet supplemented with ketoacids reduces the severity of renal disease in 5/6 nephrectomized rats: A role for KLF15. *Kidney Int* 79: 987-996, 2011.
23. Livak KJ and Schmittgen TD: Analysis of relative gene expression data using real-time quantitative PCR and the 2(-Delta Delta C(T)) method. *Methods* 25: 402-408, 2001.
24. Tervaert TW, Mooyaart AL, Amann K, Cohen AH, Cook HT, Drachenberg CB, Ferrario F, Fogo AB, Haas M, de Heer E, *et al*: Renal pathology society. pathologic classification of diabetic nephropathy. *J Am Soc Nephrol* 21: 556-563, 2010.
25. Wang Y, Zhang R, Shen H, Kong J and Lv X: Pioglitazone protects blood vessels through inhibition of the apelin signaling pathway by promoting KLF4 expression in rat models of T2DM. *Biosci Rep* 39: BSR20190317, 2019.
26. Yin J, Wang Y, Chang J, Li B, Zhang J, Liu Y, Lai S, Jiang Y, Li H and Zeng X: Apelin inhibited epithelial-mesenchymal transition of podocytes in diabetic mice through downregulating immunoproteasome subunits $\beta 5i$. *Cell Death Dis* 9: 1031, 2018.
27. Abrahamson DR: Role of the podocyte (and glomerular endothelium) in building the GBM. *Semin Nephrol* 32: 342-349, 2012.
28. Lennon R, Byron A, Humphries JD, Randles MJ, Carisey A, Murphy S, Knight D, Brenchley PE, Zent R and Humphries MJ: Global analysis reveals the complexity of the human glomerular extracellular matrix. *J Am Soc Nephrol* 25: 939-951, 2014.
29. Miner JH: Type IV collagen and diabetic kidney disease. *Nat Rev Nephrol* 16: 3-4, 2020.
30. Seo K, Parikh VN and Ashley EA: Stretch-induced biased signaling in angiotensin ii type 1 and apelin receptors for the mediation of cardiac contractility and hypertrophy. *Front Physiol* 11: 181, 2020.
31. Eleftheriadis T, Antoniadi G, Pissas G, Liakopoulos V and Stefanidis I: The renal endothelium in diabetic nephropathy. *Ren Fail* 35: 592-599, 2013.
32. Swärd P and Rippe B: Acute and sustained actions of hyperglycaemia on endothelial and glomerular barrier permeability. *Acta Physiol (Oxf)* 204: 294-307, 2012.
33. Jaimes EA, Hua P, Tian RX and Rajj L: Human glomerular endothelium: Interplay among glucose, free fatty acids, angiotensin II, and oxidative stress. *Am J Physiol Renal Physiol* 298: F125-F132, 2010.
34. Li N, Ma X, Ban T, Xu S, Ma Y, Ason B and Hu LA: Loss of APJ mediated β -arrestin signalling improves high-fat diet induced metabolic dysfunction but does not alter cardiac function in mice. *Biochem J* 477: 3313-3327, 2010.



Copyright © 2025 Huang et al. This work is licensed under a Creative Commons Attribution-NonCommercial-NoDerivatives 4.0 International (CC BY-NC-ND 4.0) License.